PUBLISHED VERSION:
A. Freddi, S. Longhi, and A. Monteriù, “A Model-Based Fault Diagnosis System for a Mini-Quadrotor,” in Proceedings of the 7th Workshop on Advanced Control and Diagnosis (ACD), pp. 1–6, Zielona Gora, Poland, Nov. 2009.

A Model-Based Fault Diagnosis System for a Mini-Quadrotor

A. Freddi, S. Longhi, A. Monteriù

Università Politecnica delle Marche, DIIGA, Ancona, Italy

Abstract: This paper addresses the problem of fault detection and isolation (FDI) for a mini-quadrotor. First a model for a four-rotor rotorcraft is presented whose model is obtained via a Lagrange approach. In order to stabilize the quadrotor at low cruise speed, a control strategy based on PD (Proportional-Derivative) controllers is presented. Using a Thau's observer, a diagnostic system has been developed for the nonlinear model of the quadrotor. Different simulation trials have been performed and the analysis of the results proves that the developed diagnostic system represents an effective solution to FDI problems in mini-flying machines.

Keywords: quadrotor dynamics, model-based fault diagnosis, fault detection, fault isolation, observers.

1. INTRODUCTION

Unmanned aerial vehicles (UAVs) or flying robots have attracted enormous interest during the last years. Recent developments in solid state disks, integrated miniature actuators and MEMS (Micro Electromechanical Systems) technology sensors have made autonomous miniaturized flying robots possible. One type of mini-aerial vehicle with a strong potential is the four-rotor aerial vehicle, also called quadrotor. This vehicle has been chosen by many researchers as a very promising vehicle for indoor/outdoor navigation using multidisciplinary concepts (Altug et al. (2002); Mokhtari and Benallegue (2004); Tayebi and McGilvray (2006); Bethke et al. (2008)). A quadrotor is an under-actuated system with four independent inputs and six coordinate outputs. The quadrotor has some advantages over conventional mini-helicopters. One of the advantages of quadrotors is that they have more lift thrusts than conventional helicopters. Moreover, they are potentially simpler to build and highly maneuverable.

Several methods have been proposed to control a quadrotor vehicle (Altug et al. (2002); Bouabdallah et al. (2004); Castillo et al. (2005); Das et al. (2009)), however only few researches have been devoted to the important problem of detecting and isolating sensor faults on a such vehicle (Berbra et al. (2008); Rafaralahy et al. (2008)). The nonlinearity of the quadrotor model does not permit to exploit the significant developments which have been made in the area of fault detection in linear systems (Chen and Patton (1999)).

The contribution of this paper is to successfully develop and apply a diagnostic observer to the nonlinear quadrotor model for detecting and isolating the rotorcraft sensor faults. Exploiting the Lipschitzianity of the nonlinear model, a full order Thau observer(Thau (1973)) is obtained and used to generate the residuals on which the FDI system is based. In faultless situations, residuals remain around zero, while if a sensor fault occurs, their values change, permitting to detect the fault. The proposed scheme permits to detect and isolate faults on the onboard inertial measurement unit (accelerometers and inclinometers).

The paper is organized as follows. In Section II, the nonlinear model of a mini-quadrotor is presented. The strategy to control the quadrotor is detailed in Section III. The proposed fault diagnostic nonlinear observer is described in Section IV. Section V is devoted to the presentation of the simulation results obtained for various fault scenarios when the proposed scheme is applied to the quadrotor. Conclusions and future directions are presented at the end of the paper.

2. DYNAMICAL MODELING OF QUADROTOR

A quadrotor simply consists in four DC motors on which propellers are fixed. These motors are arranged to the extremities of a X-shaped frame, where all the arms make an angle of 90 degrees with one another. As shown in Figure 1, the front and rear motors ($\mathcal{M}_1$ and $\mathcal{M}_3$) spin in the counter-clockwise direction with angular velocities ω_1 and ω_3, while the other two rotors ($\mathcal{M}_2$ and $\mathcal{M}_4$) spin in the clockwise direction with angular velocities ω_2 and ω_4.

The mathematical model developed here is based on some basic assumptions as given below:

- Design is symmetrical.
- Quadrotor body is rigid.
- Propellers are rigid.
- There are not external effects on quadrotor body such as air friction, wind pressure, etc.
- Free stream air velocity is zero.
- The four electric motors' dynamic is relatively fast and therefore it will be neglected as well as the flexibility of the blades.

Two frames are used to study the system motion: an inertial earth frame $\{R_E\}\,(O_E, x_E, y_E, z_E)$, and a body-fixed frame $\{R_B\}\,\{O_B, x_B, y_B, z_B\}$, where O_B is supposed

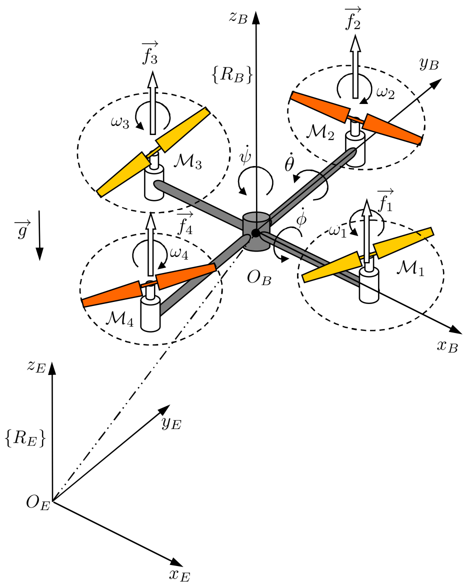

Fig. 1. Quadrotor rotorcraft.

to be at the mass center of the quadrotor. $\{R_B\}$ is related to $\{R_E\}$ by a vector $\xi = [x_E\ y_E\ z_E]^T$ describing the position of the center of gravity in $\{R_E\}$, and three independent angles $\eta = [\phi\ \theta\ \psi]^T$, which are the three Euler angles (roll, pitch and yaw angles) and describe the rotorcraft orientation, with $\left(-\frac{\pi}{2} \leq \phi < \frac{\pi}{2}\right)$, $\left(-\frac{\pi}{2} \leq \theta < \frac{\pi}{2}\right)$ and $(-\pi \leq \psi < \pi)$ (see Figure 1).

The small rotorcraft is supposed to have six degrees of freedom according to the earth fixed frame given respectively by quadrotor position and its attitude. Quadrotor is placed in the body-fixed frame $\{R_B\}\{O_B, x_B, y_B, z_B\}$ with its center of mass at O_B, and the weight force acts at this point. Weight force is always along negative z_B-axis. If l is the length of each arm, then each motor can be located by position vectors: $\boldsymbol{L}_1 = l\hat{\imath}_B$, $\boldsymbol{L}_2 = l\hat{\jmath}_B$, $\boldsymbol{L}_3 = -l\hat{\imath}_B$ and $\boldsymbol{L}_4 = -l\hat{\jmath}_B$, with $(\hat{\imath}_B, \hat{\jmath}_B, \hat{k}_B)$ as versors of (x_B, y_B, z_B)-axis. Analogously, all the forces shown in the figure by f_i $(i = 1, 2, 3, 4)$ are located from the origin O_B by position vectors $\boldsymbol{L}_i$.

With these assumptions, the quadrotor is a solid body evolving in 3D and subject to one force and three moments: moments of inertia about x_E, y_E and z_E-axis. The imbalance of the forces f_j, where $j = 1, 3$ or $j = 2, 4$, results in moments, along a direction perpendicular to the plane formed by the force f_j and the vector $\boldsymbol{L}_j$. This torque is responsible for the rotation of the machine along x-axis and y-axis. The rotation about z-axis is due to imbalance of clockwise and counter-clockwise torques.

The translational kinetic energy of the rotorcraft is expressed as (Salazar et al. (2009))

$$T_{trans} \triangleq \frac{1}{2} m \dot{\xi}^T \dot{\xi} \tag{1}$$

where m denotes the whole mass of the rotorcraft.

The rotational kinetic energy is given by

$$T_{rot} \triangleq \frac{1}{2} \dot{\eta}^T \mathbb{J} \dot{\eta} \tag{2}$$

where $\mathbb{J} \triangleq diag\,(I_{xx}, I_{yy}, I_{zz})$ is the inertia matrix expressed directly in terms of the generalized coordinates η. Due to the symmetry of the quadrotor assuming that the coupling inertia is zero, the inertia matrix is diagonal.

The only potential energy which needs to be considered is due to the gravitational force g. Therefore, potential energy is expressed as

$$U = mgz_E$$

Let $q = (x_E, y_E, z_E, \phi, \theta, \psi) \in \mathbb{R}^6$ be the generalized coordinates vector for the flying machine, the Lagrangian is given by

$$\begin{aligned} \mathcal{L}(q, \dot{q}) &= T_{trans} + T_{rot} - U \\ &= \frac{1}{2} m \dot{\xi}^T \dot{\xi} + \frac{1}{2} \dot{\eta}^T \mathbb{J} \dot{\eta} - mgz_E \end{aligned} \tag{3}$$

The model for the full quadrotor aircraft dynamics is obtained from the Euler-Lagrange equations with external generalized force

$$\frac{d}{dt} \frac{\partial \mathcal{L}}{\partial \dot{q}} - \frac{\partial \mathcal{L}}{\partial q} = F \tag{4}$$

where $F = (F_\xi, \tau)$. F_ξ defines the translational force applied to the aerial robot due to the control inputs and relative to the frame $\{R_E\}$, and τ is the generalized moments vector. The small body forces are ignored, and we only consider the principal control inputs u and τ , where u represents the total thrust, and τ is the generalized moment.

Because of each spinning propeller generates vertically upward lifting force, labeled as f_1, f_2, f_3 and f_4, all the motion of the quadrotor is a consequence of the sum of these forces:

$$u = f_1 + f_2 + f_3 + f_4 \tag{5}$$

with

$$f_i = K_l \omega_i^2 \qquad (i = 1, 2, 3, 4) \tag{6}$$

where ω_i is the angular speed of motor "i" ($\mathcal{M}_i$, $i = 1, 2, 3, 4$), while $K_l > 0$ is the lift constant depending on the air density ρ, the lift coefficient C_z and the blade rotor characteristics S (diameter, step, profile, ...) and it results as

$$K_l = \frac{1}{2} \rho S C_z \tag{7}$$

Then, the force applied to the mini-rotorcraft relative to the frame $\{R_B\}$ is defined as

$$\hat{F} = \begin{bmatrix} 0 \\ 0 \\ u \end{bmatrix} \tag{8}$$

Consequently

$$F_\xi = R_{B \to E} \hat{F} \tag{9}$$

where $R_{B \to E}$ is the rotation transformation from the body reference frame to the earth reference frame given by

$$R_{B \to E} = \begin{bmatrix} C_\theta C_\psi & C_\psi S_\theta S_\phi - C_\phi S_\psi & C_\phi C_\psi S_\theta + S_\phi S_\psi \\ C_\theta S_\psi & S_\theta S_\phi S_\psi + C_\phi C_\psi & C_\phi S_\theta S_\psi - C_\psi S_\phi \\ -S_\theta & C_\theta S_\phi & C_\theta C_\phi \end{bmatrix}$$

where $S_{(.)}$ and $C_{(.)}$ represent $\sin(.)$ and $\cos(.)$ respectively.

The generalized moments on the η variables are

$$\tau \triangleq \begin{bmatrix}\tau_\phi \\ \tau_\theta \\ \tau_\psi\end{bmatrix} = \begin{bmatrix}(f_4 - f_2)\, l \\ (f_3 - f_1)\, l \\ \sum_{j=1}^{4} \tau_{\mathcal{M}_j}\end{bmatrix} \tag{10}$$

where l is the distance from any internal motor to the centre of gravity and $\tau_{\mathcal{M}_j}$ is the couple produced by motor $\mathcal{M}_j$.

Therefore, the Euler-Lagrange equation can be rewritten as

$$m\ddot{\xi} + \begin{bmatrix}0 \\ 0 \\ mg\end{bmatrix} = F_\xi \tag{11}$$

$$\mathbb{J}\ddot{\eta} + \dot{\mathbb{J}}\dot{\eta} - \frac{1}{2}\frac{\partial}{\partial\eta}\left(\dot{\eta}^T\mathbb{J}\dot{\eta}\right) = \tau \tag{12}$$

Defining the Coriolis vector as

$$F_c(\eta,\dot{\eta}) = \dot{\mathbb{J}} - \frac{1}{2}\frac{\partial}{\partial\eta}\left(\dot{\eta}^T\mathbb{J}\right) \tag{13}$$

the expression (12) can be rewritten as

$$\mathbb{J}\ddot{\eta} + F_c(\eta,\dot{\eta})\,\dot{\eta} = \tau \tag{14}$$

Finally, the equations of motion for the mini rotorcraft are expressed as

$$m\ddot{\xi} = F_\xi + \begin{bmatrix}0 \\ 0 \\ -mg\end{bmatrix} \tag{15}$$

$$\mathbb{J}\ddot{\eta} = \tau - F_c(\eta,\dot{\eta})\,\dot{\eta} \tag{16}$$

Since $\mathbb{J}$ is nonsingular, it is possible to simplify the analysis changing the input variables as follows

$$\tau = \mathbb{J}\tilde{\tau} + F_c(\eta,\dot{\eta})\,\dot{\eta} \tag{17}$$

where

$$\tilde{\tau} = \begin{bmatrix}\tilde{\tau}_\phi \\ \tilde{\tau}_\theta \\ \tilde{\tau}_\psi\end{bmatrix} \tag{18}$$

are the new inputs. Then

$$\ddot{\eta} = \tilde{\tau} \tag{19}$$

Rewriting (15) and (16) gives

$$m\ddot{x} = u(C_\phi C_\psi S_\theta + S_\phi S_\psi) \tag{20}$$
$$m\ddot{y} = u(C_\phi S_\theta S_\psi - C_\psi S_\phi) \tag{21}$$
$$m\ddot{z} = u(C_\theta C_\phi) - mg \tag{22}$$
$$\ddot{\phi} = \tilde{\tau}_\phi \tag{23}$$
$$\ddot{\theta} = \tilde{\tau}_\theta \tag{24}$$
$$\ddot{\psi} = \tilde{\tau}_\psi \tag{25}$$

3. CONTROL STRATEGY

A control strategy for stabilizing the quadrotor near hover is presented in this section. The control input u is essentially used to make the altitude reach a desired value. The control input $\tilde{\tau}_\psi$ is used to set the yaw displacement to zero. $\tilde{\tau}_\theta$ is used to control the pitch angle and the horizontal movement in the x_E-axis. Similarly $\tilde{\tau}_\phi$ is used to control the roll angle and the horizontal displacement in the y_E-axis (Castillo et al. (2005)).

3.1 Altitude control

The control of the vertical position can be obtained by using the following control input (Salazar et al. (2009))

$$u = -m\sigma_b\left(b_{z_1}\dot{z}_E + b_{z_2}(z_E - z_d)\right) + mg \tag{26}$$

where b_{z_1}, b_{z_2} are positive constant and z_d is the desired altitude.

3.2 Attitude control

The control of the attitude can be obtained by using the following PD controllers (Salazar et al. (2009))

$$\tilde{\tau}_\psi = \sigma_a\left(-a_{\psi_1}\dot{\psi} - a_{\psi_2}(\psi - \psi_d)\right) \tag{27}$$
$$\tilde{\tau}_\theta = \sigma_a\left(-a_{\theta_1}\dot{\theta} - a_{\theta_2}\theta\right) \tag{28}$$
$$\tilde{\tau}_\phi = \sigma_a\left(-a_{\phi_1}\dot{\phi} - a_{\phi_2}\phi\right) \tag{29}$$

where $\sigma_a(s)$ is a saturation function defined as

$$\sigma_a(s) = \begin{cases} a, & \text{if } s > a \\ s, & \text{if } -a \le s \le a \\ -a, & \text{if } s < -a \end{cases} \tag{30}$$

Introducing the control law in the model

$$\ddot{\psi} = \sigma_a\left(-a_{\psi_1}\dot{\psi} - a_{\psi_2}(\psi - \psi_d)\right) \tag{31}$$
$$\ddot{\theta} = \sigma_a\left(-a_{\theta_1}\dot{\theta} - a_{\theta_2}\theta\right) \tag{32}$$
$$\ddot{\phi} = \sigma_a\left(-a_{\phi_1}\dot{\phi} - a_{\phi_2}\phi\right) \tag{33}$$

where $a_{\psi_1}, a_{\psi_2}, a_{\theta_1}, a_{\theta_2}, a_{\phi_1}$ and a_{ϕ_2} are positive constants which should be carefully chosen to obtain a stable well-damped response.

4. FDI SYSTEM

In literature several model-based methods have been adopted for generating residual to be used in FDI schemes for UAVs. Luenberger observers have been used both for sensor and actuator fault detection (see Heredia et al. (2007)). Kalman filters (simple, extended or unscented) have been used for fault adaptive and tolerant control (see, e.g., Qi et al. (2007) and Rago et al. (1998)).

Most of the times the easiest and practical solution when dealing with model-based techniques is to choose a proper working point and linearize the system around it. However this solution is suitable only for those vehicles operating most of the time near the considered conditions. In all the other cases there are two possible alternatives: linearizing the system around different operating conditions or using a non linear model-based approach.

In the present work a non-linear observer is adopted. In order to develop the observer it is necessary to write the system described by the equations (20)-(25) in a state-space form. Defining $\boldsymbol{x} = [x_E\ y_E\ z_E\ \phi\ \theta\ \psi\ \dot{x}_E\ \dot{y}_E\ \dot{z}_E\ \dot{\phi}\ \dot{\theta}\ \dot{\psi}]^T$ as the state vector, $\boldsymbol{u} = [\tilde{\tau}_\phi\ \tilde{\tau}_\theta\ \tilde{\tau}_\psi\ ]^T$ as the input vector and $\boldsymbol{y} = [x_E\ y_E\ z_E\ \phi\ \theta\ \psi\ ]^T$ as the output vector, then the system described in eq. (20)-(25) can be rewritten as

$$\begin{cases}\dot{\boldsymbol{x}}(t) = \boldsymbol{A}\boldsymbol{x}(t) + \boldsymbol{B}\boldsymbol{u}(t) + \boldsymbol{h}(\boldsymbol{x}(t),\boldsymbol{u}(t)) \\ \boldsymbol{y}(t) = \boldsymbol{C}\boldsymbol{x}(t)\end{cases} \tag{34}$$

where

$$\boldsymbol{A} = \begin{bmatrix} 0&0&0&0&0&0&1&0&0&0&0&0 \\ 0&0&0&0&0&0&0&1&0&0&0&0 \\ 0&0&0&0&0&0&0&0&1&0&0&0 \\ 0&0&0&0&0&0&0&0&0&1&0&0 \\ 0&0&0&0&0&0&0&0&0&0&1&0 \\ 0&0&0&0&0&0&0&0&0&0&0&1 \\ 0&0&0&0&0&0&0&0&0&0&0&0 \\ 0&0&0&0&0&0&0&0&0&0&0&0 \\ 0&0&0&0&0&0&0&0&0&0&0&0 \\ 0&0&0&0&0&0&0&0&0&0&0&0 \\ 0&0&0&0&0&0&0&0&0&0&0&0 \\ 0&0&0&0&0&0&0&0&0&0&0&0 \end{bmatrix}, \tag{35}$$

$$\boldsymbol{B} = \begin{bmatrix} 0&0&0&0&0&0&0&0&0&0&0&0 \\ 0&0&0&0&0&0&0&0&0&1&0&0 \\ 0&0&0&0&0&0&0&0&0&0&1&0 \\ 0&0&0&0&0&0&0&0&0&0&0&1 \end{bmatrix}^T, \tag{36}$$

$$\boldsymbol{C} = \begin{bmatrix} 1&0&0&0&0&0&0&0&0&0&0&0 \\ 0&1&0&0&0&0&0&0&0&0&0&0 \\ 0&0&1&0&0&0&0&0&0&0&0&0 \\ 0&0&0&1&0&0&0&0&0&0&0&0 \\ 0&0&0&0&1&0&0&0&0&0&0&0 \\ 0&0&0&0&0&1&0&0&0&0&0&0 \end{bmatrix}, \tag{37}$$

and

$$\boldsymbol{h}(\boldsymbol{x}, \boldsymbol{u}) = \begin{bmatrix} (C_\phi C_\psi S_\theta + S_\phi S_\psi) \\ (C_\phi S_\theta S_\psi - C_\psi S_\phi) \\ (C_\theta C_\phi) \end{bmatrix} \boldsymbol{u} - \begin{bmatrix} 0 \\ 0 \\ g \end{bmatrix}. \tag{38}$$

A suitable observer for this kind of system is the observer proposed in Thau (1973). This observer has already been applied to the fault detection and isolation of non-linear dynamic systems and uses the following non-linear system model (Chen and Patton (1999)):

$$\begin{cases} \dot{\boldsymbol{x}}(t) = \boldsymbol{A}\boldsymbol{x}(t) + \boldsymbol{B}\boldsymbol{u}(t) + \boldsymbol{h}(\boldsymbol{x}(t), \boldsymbol{u}(t)) + \boldsymbol{F_1}\boldsymbol{f}(t) \\ \boldsymbol{y}(t) = \boldsymbol{C}\boldsymbol{x}(t) + \boldsymbol{F_2}\boldsymbol{f}(t) \end{cases} \tag{39}$$

where $\boldsymbol{F_1}$ and $\boldsymbol{F_2}$ are known as fault entry matrices which represent the effect of faults on the system.

The system model has to satisfy the two following conditions:

C1, the pair $(\boldsymbol{C}, \boldsymbol{A})$ must be observable;
C2, the non-linear function $\boldsymbol{h}(\boldsymbol{x}(t), \boldsymbol{u}(t))$ must be continuously differentiable and locally Lipschitz with constant ϱ, i.e.

$$||\boldsymbol{h}(\boldsymbol{x_1}(t), \boldsymbol{u}(t)) - \boldsymbol{h}(\boldsymbol{x_2}(t), \boldsymbol{u}(t))|| \leq \varrho||(\boldsymbol{x_1} - \boldsymbol{x_2})|| \tag{40}$$

When these two conditions are satisfied, a stable observer for the system (39) can be constructed as

$$\begin{cases} \dot{\hat{\boldsymbol{x}}}(t) = \boldsymbol{A}\hat{\boldsymbol{x}}(t) + \boldsymbol{B}\boldsymbol{u}(t) + \boldsymbol{h}(\hat{\boldsymbol{x}}(t), \boldsymbol{u}(t)) + \boldsymbol{K}(\boldsymbol{y}(t) - \hat{\boldsymbol{y}}(\boldsymbol{t})) \\ \hat{\boldsymbol{y}}(t) = \boldsymbol{C}\hat{\boldsymbol{x}}(t) \end{cases} \tag{41}$$

where $\boldsymbol{K}$ is the observer gain matrix defined by

$$\boldsymbol{K} = \boldsymbol{P_\theta}^{-1} C^T \tag{42}$$

The matrix $\boldsymbol{P_\theta}$ is the solution to the Lyapunov equation

$$\boldsymbol{A}^T\boldsymbol{P_\theta} + \boldsymbol{P_\theta}\boldsymbol{A} - \boldsymbol{C}^T\boldsymbol{C} + \theta\boldsymbol{C}^T\boldsymbol{P_\theta} = 0 \tag{43}$$

where θ is a positive parameter which is chosen such that (43) has a positive definite solution.

In this case of study the pair $(\boldsymbol{C}, \boldsymbol{A})$ is observable and the first condition is satisfied. Since $\boldsymbol{h}(\boldsymbol{x}(t), \boldsymbol{u}(t))$ is a function with only sine and cosine non-linearities, it results continuously differentiable and thus the condition **C2** is satisfied as long as $\boldsymbol{u}$ is properly chosen. The parameter θ has been chosen in order to maximize the effect of faults on the residuals while keeping the detection time small.

The gain matrix used for the simulations is:

$$\boldsymbol{K} = \begin{bmatrix} 1.1 & 0 & 0 & 0 & 0 & 0 \\ 0 & 1.1 & 0 & 0 & 0 & 0 \\ 0 & 0 & 1.1 & 0 & 0 & 0 \\ 0 & 0 & 0 & 1.1 & 0 & 0 \\ 0 & 0 & 0 & 0 & 1.1 & 0 \\ 0 & 0 & 0 & 0 & 0 & 1.1 \\ 0.3025 & 0 & 0 & 0 & 0 & 0 \\ 0 & 0.3025 & 0 & 0 & 0 & 0 \\ 0 & 0 & 0.3025 & 0 & 0 & 0 \\ 0 & 0 & 0 & 0.3025 & 0 & 0 \\ 0 & 0 & 0 & 0 & 0.3025 & 0 \\ 0 & 0 & 0 & 0 & 0 & 0.3025 \end{bmatrix} \tag{44}$$

5. SIMULATION RESULTS

The non-linear quadrotor system along with the FDI system have been developed using the Matlab and Simulink® software. The nonlinear system outputs are supposed to be the position in the earth frame (x_E, y_E and z_E) and the euler angles (ϕ, θ and ψ). The residuals (six) are built as the difference between the nonlinear system outputs and the Thau observer outputs. They are supposed to be zero as long as there are no faults on the sensors and to differ from zero in case of faults.

Sensors used in autonomous helicopters can fail in several ways (Heredia et al. (2007)). Some failure types are general for various sensors, while others are specific of a single sensor.

The faults simulated in the present paper are additive and of two different kinds: abrupt (step-like faults) and incipient (ramp-like faults).

First a fault-free simulation in which the quadrotor must follow a desired trajectory is performed. The trajectory implies:

- vertical flight for $25m$ in the positive direction(take-off);
- lateral flight for $15m$ in the positive direction;
- longitudinal flight for $15m$ in the positive direction;
- lateral flight for $15m$ in the negative direction;
- longitudinal flight for $15m$ in the negative direction;
- vertical flight for$25m$ in the negative direction (landing).

This closed trajectory is well followed by the vehicle as long as there is no fault on the sensors, as it can be seen in Fig. 2.

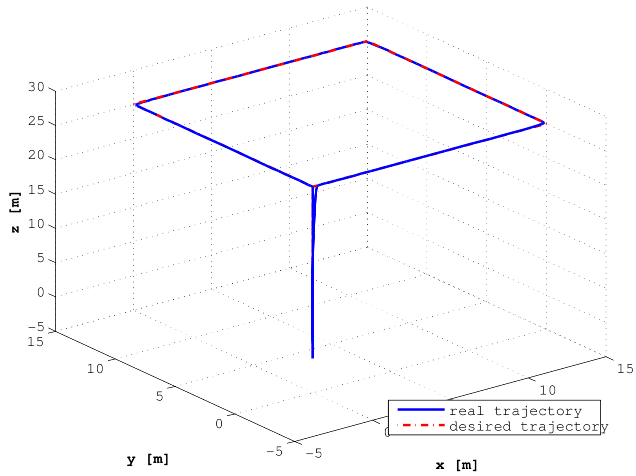

Fig. 2. Quadrotor fault-free trajectory.

Then the system is tested in case of faults. All the faults are introduced at $75s$ of the simulation, that is to say while the quadcopter is performing the backward lateral trajectory.

5.1 Faults on the Accelerometers

The first fault is abrupt and on the longitudinal accelerometer.

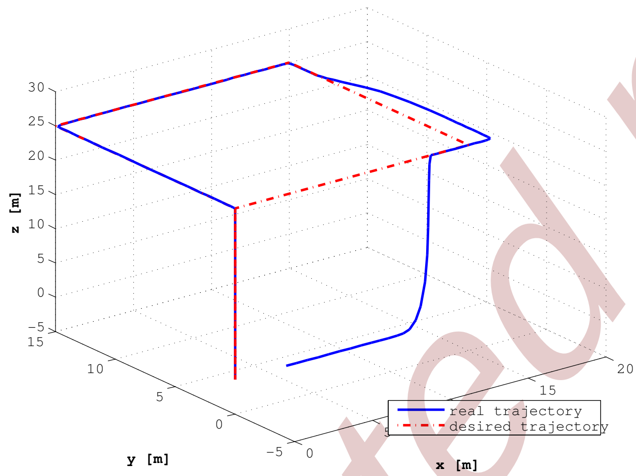

Fig. 3. Quadrotor trajectory in case of fault on the longitudinal accelerometer.

As it can be seen in Fig. 3, the quadcopter stops following the trajectory when the fault occurs and in case of no change in the controller strategy it would crash to the ground. However the first residual of the FDI system is sensitive to this kind of faults as it is shown in Fig. 4.

The second kind of tested fault is incipient. Even in this case the first residual is sensitive to the fault on the longitudinal accelerometer and allows its isolation (Fig. 5).

The behavior of the system in case of faults on the two other accelerometers is identical, thus it is not described for brevity.

5.2 Faults on the Inclinometers

The first fault is abrupt and on the ϕ inclinometer.

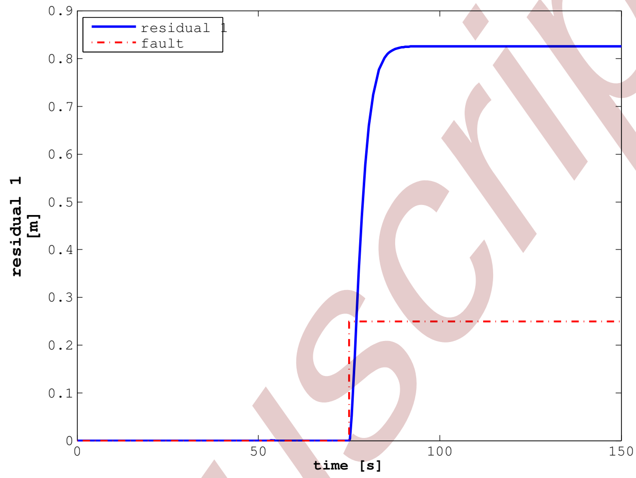

Fig. 4. Residual 1 in case of abrupt fault on the longitudinal accelerometer.

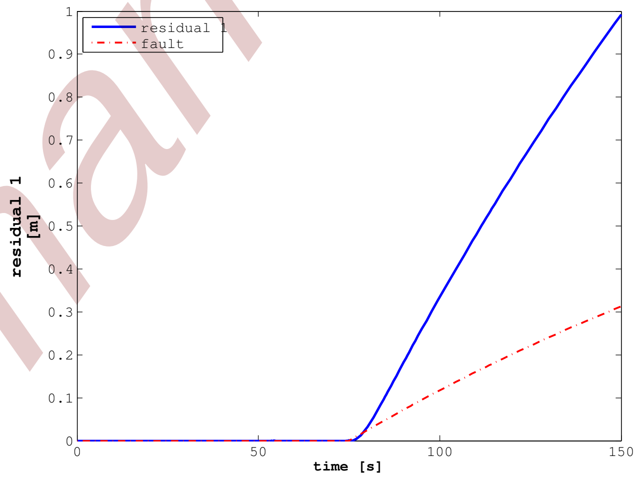

Fig. 5. Residual 1 in case of incipient fault on the longitudinal accelerometer.

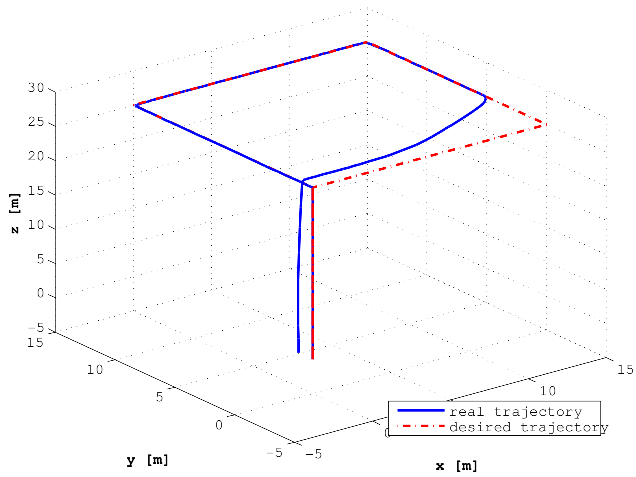

Fig. 6. Quadrotor trajectory in case of fault on the ϕ inclinometer.

As it can be seen in Fig. 6, the quadcopter stops following the trajectory when the fault occurs similarly as in the previous case, however the results is that it lands in a point far from that designated by the controller, rather than crashing to the ground. In this case it is the second residual of the FDI system to be sensitive to this kind of fault as it is shown in Fig. 7.

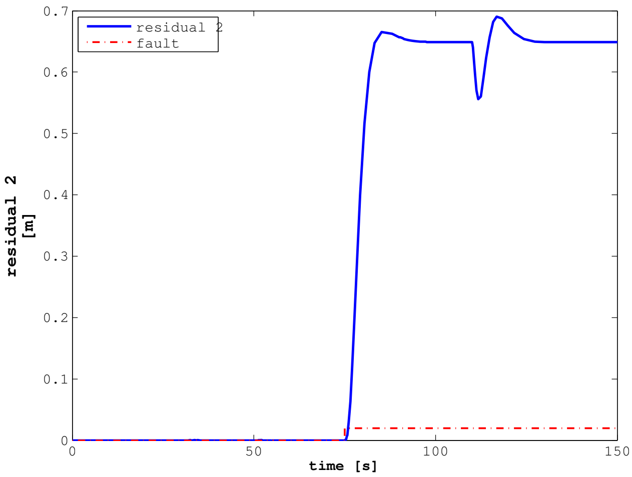

Fig. 7. Residual 2 in case of abrupt fault on the ϕ accelerometer.

The second kind of tested fault is incipient. Even in this case the second residual is sensitive to the fault on the ϕ accelerometer and allows its isolation (Fig. 8).

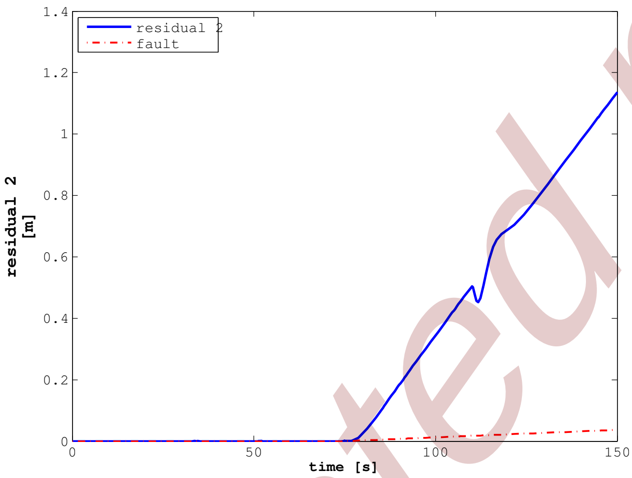

Fig. 8. Residual 4 in case of incipient fault on the ϕ inclinometer.

The behavior of the system in case of faults on the θ inclinometer is identical, thus it is not described for brevity.

In real quadcopters there is always a built-in yaw controller that is necessary to stabilize the yaw movement. Without this stabilization there is no possible flight. The developed controller simulates this situation as the yaw control is the first and fastest to be performed in the loop chain. Due to this situation, any fault on the yaw inclinometer is almost immediately corrected by the controller and cannot be detected. However this behaviour causes no problem in real applications because the yaw controller is most of the time integrated and a fault on it would make the vehicle almost impossible to further control.

6. CONCLUDING REMARKS

In this paper, the FDI problem for a quadrotor vehicle has been faced. Using a Thau's observer, a set of residuals have been generated for FDI tasks. Simulation trials have shown that accelerometers and inclinometers faults can be correctly detected and isolated. A strategy for disturbance reduction and fault tolerant control is currently under investigation.

REFERENCES

Altug, E., Ostrowski, J., and Mahony, R. (2002). Control of a quadrotor helicopter using visual feedback. In *Proc. of IEEE Int. Conf. on Robotics and Automation*.

Berbra, C., Lesecq, S., and Martinez, J. (2008). A multi-observer switching strategy for fault-tolerant control of a quadrotor helicopter. 1094–1099.

Bethke, B., Valenti, M., and How, J. (2008). Uav task assignment. *IEEE Trans. on Robotics and Automation*, 15(1), 39–44.

Bouabdallah, S., Murrieri, P., and Siegwart, R. (2004). Design and control of an indoor micro quadrotor. 4393–4398.

Castillo, P., Lozano, R., and Dzul, A. (2005). *Modelling and control of mini-flying machines*. Springer-Verlag.

Chen, J. and Patton, R. (1999). *Robust model-based fault diagnosis for dynamic systems*.

Das, A., Subbarao, K., and Lewis, F. (2009). Dynamic inversion with zero-dynamics stabilisation for quadrotor control. *IET Contr. Theory & Applications*, 303–314.

Heredia, G., Ollero, A., Bejar, M., and Mahtani, R. (2007). Sensor and actuator fault detection in small autonomous helicopters. *Mechatronics*.

Mokhtari, A. and Benallegue, A. (2004). Dynamic feedback controller of euler angles and wind parameters estimation for a quadrotor unmanned aerial vehicle.

Qi, J., Jiang, Z., Zhao, X., and Han, J. (2007). UKF-based rotorcraft UAV Fault adaptive control for actuator failure. In *IEEE International Conference on Robotics and Biomimetics, 2007. ROBIO 2007*, 1545–1550.

Rafaralahy, H., Richard, E., Boutayeb, M., and Zasadzinski, M. (2008). Simultaneous observer based sensor diagnosis and speed estimation of unmanned aerial vehicle. 2938–2943.

Rago, C., Prasanth, R., Mehra, R., Fortenbaugh, R., Inc, S., and Woburn, M. (1998). Failure detection and identification and fault tolerant controlusing the IMM-KF with applications to the Eagle-Eye UAV. In *Proc. of the 37th IEEE Conf. on Decision and Control*.

Salazar, S., Romero, H., Lozano, R., and Castillo, P. (2009). Modeling and real-time stabilization of an aircraft having eight rotors. *Journal of Intelligent and Robotic Systems*, 54(1), 455–470.

Tayebi, A. and McGilvray, S. (2006). Attitude stabilization of a vtol quadrotor aircraft. *IEEE Transactions on Control Systems Technology*, 14(3), 562–571.

Thau, F. (1973). Observing the state of non-linear dynamic systems. *Int. Jour. of Control*, 17(3), 471–479.